International Journal of Technical Innovation in Modern Engineering & Science (IJTIMES)
Impact Factor: 3.45 (SJIF-2015), e-ISSN: 2455-2585
Volume 4, Issue 01, January-2018

NUMERICAL INVESTIGATIONS ON SUPERSONIC FLUID FLOW BEHAVIORS PAST A CAVITY CONCERNING VELOCITY FIELD AND AEROACOUSTIC INFLUENCES WITH LES-APPROACH

Dr. Nirmal Kumar Kund

Associate Professor, Department of Production Engineering
Veer Surendra Sai University of Technology, Burla 768018, India

Abstract— A suitable numerical model is developed to predict supersonic flow pertaining to a 3D open cavity. The researches of supersonic flow over the 3D cavity having length-to-depth ratio of 2, include the supersonic free-stream Mach number of 2 and the flow Reynolds number of 10^5. The numerical simulation has been done with the Large Eddy Simulation (LES) approach. The Smagorinky model is introduced for the present investigation. The results found have been compared with the numerical simulation predictions available in the literature. The results have been expressed in the form of both coefficient of pressure (Cp) and overall sound pressure level (OASPL) along the side wall of the open cavity. The coefficient of pressure along the side wall of the said cavity appears to be very much comparable both qualitatively and quantitatively with the reported numerical results by the other investigator. Nevertheless, the overall sound pressure level along the side wall of the stated cavity is over-predicted by nearly 25-40 dB between the aft and front walls. Above and beyond, the velocity vector pertaining to the open cavity has also been investigated. Fairly large recirculation is witnessed inside the cavity and therefore these need to be supressed. Besides, the amalgamation of a spoiler is also planned for future to alter the flow structures inside the cavity which can bring about the reduction in recirculation in addition to the overall sound pressure level along the side wall of the open cavity.

Keywords— Numerical, Cavity, LES, Coefficient of Pressure, OASPL, Side Wall.

I. INTRODUCTION

Noise generated by a flow is a major problem in many engineering applications like military vehicles, submarines, aircrafts, automobiles, etc. It can cause discomfort to humans and also affect the stealth of operations/performances. Airframe noise is a considerable component of overall noise, particularly during landing and take-off. Noise from landing gear, flaps, slats etc. are regarded as airframe noise. One of the most significant airframe noises is the cavity noise. They arise from open wheel wells after the undercarriage during landing. The weapon bays in the military aircrafts experience oscillations induced by the flow, which can excite the vibrational modes of the structure of the aircraft. At low Mach numbers for ground transportation, the automobile company is bothered with the noises generated from the door gaps, side mirrors, and the open sun roof. These noises groups also influence the ease in the vehicle.

The weapon bays, wheel wells and door gaps can be modelled as rectangular cavities and the composed flow outside the cavity can be regarded to be uniform. Though the rectangular cavity is elementary in shape, it is rich in diverse dynamic and acoustic phenomena, obscured by a possible aeroacoustic feedback loop depending on the shape/size of the cavity as well as the flow conditions. Very severe tone noises may be produced because of the vortex shredding at the upstream edge of the cavity, all through the flow past a cavity.

Heller et al. [1] examined on flow-induced pressure oscillations in shallow cavities. Tam and Block [2] studied on the tones and pressure oscillations induced by flow over rectangular cavities. Kaufman et al. [3] reported on Mach 0.6 to 3.0 flows over rectangular cavities. Sweby [4] applied high resolution schemes using flux limiters on hyperbolic conservation laws. Rizzetta [5] performed numerical simulation on supersonic flow over a three-dimensional cavity. Anderson and Wendt [6] described about the fundamentals of computational fluid dynamics. Piomelli [7] demonstrated on achievements and challenges of large-eddy simulation. Hamed et al. [8] conducted numerical simulations of fluidic control for transonic cavity flows. Li et al. [9] carried out LES study of feedback-loop mechanism of supersonic open cavity flows. Vijayakrishnan [10] executed a validation study on unsteady RANS computations of supersonic flow over two dimensional cavity. Sousa et al. [11] discussed about the lid-driven cavity flow of viscoelastic liquids**.** Tuerke et al. [12] illustrated experimental study on double-cavity flow. It is realized that an extensive study on cavity flow has been done both experimentally and computationally for improving the aerodynamic performance. Nevertheless, besides its importance, the complicated flow physics of flow past a cavity has fascinated the researchers around the globe for further investigations and remains to be a cutting-edge area of investigation.

Albeit, the flow past a cavity has been investigated both experimentally and numerically by many investigators, nevertheless, overall modelling of both large and small scales of motions, not yet accomplished which is one of the most important weaknesses. But, Large Eddy Simulation (LES) is the method which resolves the large eddies as it is and models the small eddies that can give reasonably more realistic results too. The purpose of this investigation is to study the flow physics and modes of oscillations in a 3D open cavity supersonic flow. It involves details about the governing equations and the development along with the implementation of the LES technique including the sub-grid scale modelling. The discretization procedures have also been described. The simulation results have been expressed in the form of velocity vector, coefficient of pressure (Cp) and overall sound pressure level (OASPL) along the side wall of the open cavity. The simulation predictions of supersonic flow over the open cavity have also been compared with the numerical results reported in the literature. As a whole, quite good agreement between the above stated results is also found from the current researches. Nevertheless, the studies pertaining to the use of passive control techniques/devices for the reduction of recirculation inside the cavity is planned for future. These devices operate over a wide range of parameters and hence significantly influence the flow physics of incoming boundary layer for spreading favourable flow circumstances.

II. DESCRIPTION OF PHYSICAL PROBLEM

Supersonic flow past a three-dimensional cavity is studied numerically. The streamwise length, depth and spanwise length of the cavity are 20 mm, 10 mm, and 10 mm, respectively. The length-to-depth ratio (L/D) for the cavity is 2. The width-to-depth ratio (W/D) is 1. The cavity is three-dimensional with streamwise length-to-spanwise length ratio (L/W) > 1. In addition, the Mach number of the free-stream along with the Reynolds number based on the cavity depth are taken as 2 and 10^5, respectively, for setting the inflow conditions.

2.1. Geometric Model

The computational domain of the cavity used in the present simulation is shown in figure 1. The size of the computational domain, as mentioned earlier, is 2D×D×D (length × breadth × width). The inlet boundary is located at a distance of D upstream from the leading edge of the cavity. The outlet boundary is located at a distance of 4D downstream from the trailing edge of the cavity. The upper boundary is also located at a distance of 4D above the cavity.

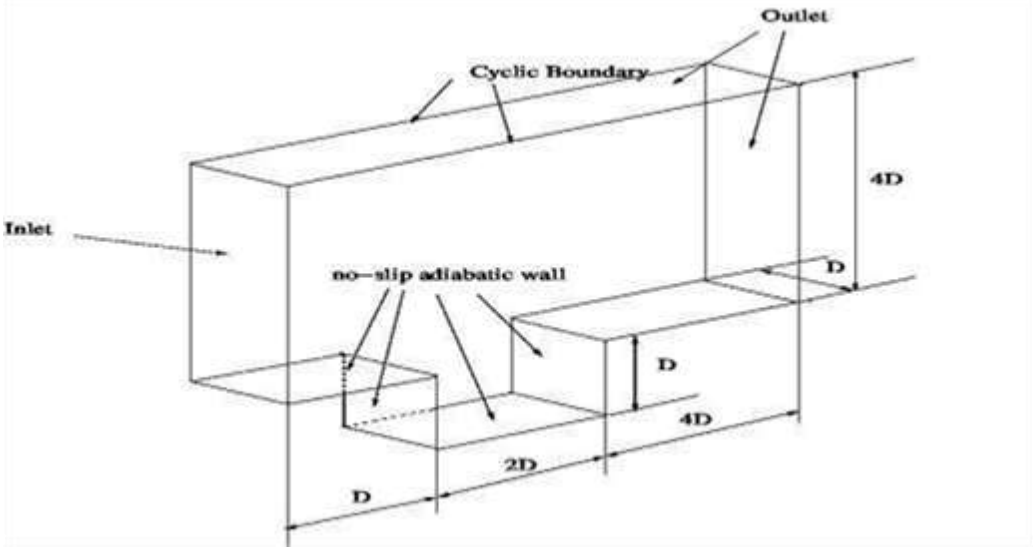

Fig 1. Computational domain of cavity

2.2. Initial and Boundary Conditions

The inflow boundary conditions are initialized with free-stream conditions of $M_\infty = 2$, $P_\infty = 101.325$ kPa, and $T_\infty = 300$ K. The Reynolds number of the flow used in the simulation is 10^5, which is based on the cavity depth. No-slip adiabatic wall boundary conditions is applied at the wall boundaries. Zero-gradient condition is applied at all the outflow boundaries. Periodical boundary condition is applied in the spanwise direction of the cavity.

III. MATHEMATICAL FORMULATION

3.1. Generalized Governing Transport Equations

The three-dimensional compressible Navier-Stokes equations are the governing equations which include the continuity equation (1), the momentum equation (2), and the energy equation (3) which are as follows:

$$\frac{\partial \rho}{\partial t} + \nabla.(\rho \boldsymbol{U}) = 0 \quad (1)$$

$$\frac{\partial (\rho \boldsymbol{U})}{\partial t} + \nabla.(\rho \boldsymbol{U}.\boldsymbol{U}) - \nabla.\nabla(\mu \boldsymbol{U}) = -\nabla p \quad (2)$$

$$\frac{\partial (\rho e)}{\partial t} + \nabla.(\rho e \boldsymbol{U}) - \nabla.\nabla(\mu e) = -p(\nabla.\boldsymbol{U}) + \mu \left[\frac{1}{2}(\nabla \boldsymbol{U} + \nabla \boldsymbol{U}^{\mathrm{T}})\right]^2 \quad (3)$$

Where,

$\boldsymbol{U}$ = velocity vector = $u\hat{\imath} + v\hat{\jmath} + w\hat{k}$

$\frac{1}{2}(\nabla \boldsymbol{U} + \nabla \boldsymbol{U}^{\mathrm{T}})$ = strain rate tensor.

The equations (1), (2) and (3) represent the conservation form of the Navier-Stokes equations. The conservation form of these governing equations are achieved from a flow model fixed in space [6]. The above equations are applicable to viscous flow, except that the mass diffusion is no included.

It is assumed, in aerodynamics, that the gas is a perfect gas. The equation of state for a perfect gas is, $p = \rho RT$ (4)

Where, R = specific gas constant = C_p - C_v (5)

For a calorically perfect gas (constant specific heats), the caloric equation of state is,

e = internal energy per unit mass = C_vT (6)

3.2. LES Turbulence Modelling

The turbulent flows may be simulated using three different approaches: Reynolds-Averaged Navier-Stokes equations (RANS), direct numerical simulation (DNS), and large eddy simulation (LES). Direct numerical simulation has high computational requirements. DNS resolves all the scales of motion and for this it needs a number of grid points proportional to $(Re)^{9/4}$ and computational scales' cost is proportional to $(Re)^3$ [7].

In the present study, features of the turbulent flow field have been simulated using LES as it is appropriate for unsteady complex flows as well as noise induced flows. LES computes the large resolved scales and also models the smallest scales. The turbulence model is introduced by splitting the time and space varying flow variables into two constituents, the resolved one $\bar{f}$ and f', the unresolved part:

$(x,t) = \bar{f}(x,t) + f'(x,t)$ (7)

LES uses a filtering operation to separate these resolved scales from the unresolved scales. The filtered variable is denoted by an over bar [7]. The top-hat filter smooth both the fluctuations of the large-scale and those of small scales as well. The filtering operation when applied to the Navier-Stokes equation gives:

$$\frac{\partial \bar{\rho}}{\partial t} + \nabla.(\overline{\rho \boldsymbol{U}}) = 0 \quad (8)$$

$$\frac{\partial (\overline{\rho \boldsymbol{U}})}{\partial t} + \nabla.(\overline{\rho \boldsymbol{U}.\boldsymbol{U}}) - \nabla.\nabla(\overline{\mu \boldsymbol{U}}) = -\nabla \bar{p} \quad (9)$$

$$\frac{\partial (\overline{\rho e})}{\partial t} + \nabla.(\overline{\rho \boldsymbol{U} e}) - \nabla.\nabla(\overline{\mu e}) = -\overline{p(\nabla.\boldsymbol{U})} + \mu \left[\frac{1}{2}(\nabla \bar{\boldsymbol{U}} + \nabla \bar{\boldsymbol{U}}^{\mathrm{T}})\right]^2 \quad (10)$$

However, the dissipative scales of motion are rectified poorly by LES. In a turbulent flow, the energy from the large resolved structures are passed on to the smaller unresolved structures by an inertial and an effective inviscid mechanism. This is known as energy cascade. Hence, LES employs a sub-grid scale model to mimic the drain related to this energy cascade. Most of these models are eddy viscosity models relating the subgrid-scale stresses (τ_{ij}) and the resolved-scale rate of strain-tensor ($\bar{S}_{ij}$),

$\tau_{ij} - (\delta_{ij}/3) = -2\nu_T \bar{S}_{ij}$ (11)

Where, $\bar{S}_{ij}$ is the resolved-scale rate of strain tensor = $(\partial \bar{u}_i/\partial x_j + \partial \bar{u}_j/\partial x_i)/2$.

In most of the cases it is assumed that all the energy received by the unresolved-scales are dissipated instantaneously. This is the equilibrium assumption, i.e., the small-scales are in equilibrium [7]. This simplifies the problem to a great extent and an algebraic model is obtained for the eddy viscosity:

$$\mu_{sgs} = \rho C\Delta^2|\bar{S}|\bar{S}_{ij},\ |\bar{S}| = (2\bar{S}_{ij}\bar{S}_{ij})^{1/2} \quad (12)$$

Here, Δ is the grid size and is usually taken to be the cube root of the cell volume [7]. This model is called as the Smagorinsky model and C is the Smagorinsky coefficient. In the present study, its value has been taken to be 0.2.

IV. NUMERICAL PROCEDURES

4.1. Numerical Scheme and Solution Algorithm

The three-dimensional compressible Navier-Stokes governing transport equations are discretized through a framework pertaining to finite volume method (FVM) using the SIMPLER algorithm. Here, the turbulent model used for large eddy simulation is Smagorinsky model, because of its simplicity. The spatial derivatives such as Laplacian and convective terms are computed by second order scheme based on Gauss theorem. In addition, the viscous terms are evaluated by second order scheme. Furthermore, the implicit second order scheme is used for time integration. The numerical fluxes are evaluated by applying Sweby limiter to central differencing (CD) scheme, which is a total variation diminishing (TVD) scheme. The central differencing (CD) is an unbounded second order scheme, whereas, the total variation diminishing (TVD) is a limited linear scheme. The established solver is used to predict flow behaviours of the associated flow variables relating to supersonic flow over an open cavity.

4.2. Choice of Grid Size, Time Step and Convergence Criteria

Figure 2 demonstrates that the computational domain comprises of two regions: upper cavity region and inside cavity region. The grid is refined at the regions near to the wall (where very high gradient is expected) to determine the behaviour of shear layer satisfactorily. A comprehensive grid-independence test is performed to establish a suitable spatial discretization, and the levels of iteration convergence criteria to be used. As an outcome of this test, the optimum number of grid points used for the final simulation, in the upper cavity region as 360 × 150 × 1 and those of in the inside cavity region as 200 × 150 × 1. Thus, the total number of grid points is 84000. The values of ΔX^+, ΔY^+ and ΔZ^+ at the leading edge of the cavity are 5, 12.5 and 1.0, respectively. Corresponding time step taken in the simulation is 0.000001 seconds. Though, it is checked with smaller grids of 132000 in numbers, it is observed that a finer grid system does not alter the results significantly.

Convergence in inner iterations is declared only when the condition $\left|\frac{\varphi-\varphi_{old}}{\varphi_{max}}\right| \leq 10^{-4}$ is satisfied simultaneously for all variables, where φ stands for the field variable at a grid point at the current iteration level, φ_{old} represents the corresponding value at the previous iteration level, and φ_{max} is the maximum value of the variable at the current iteration level in the entire domain.

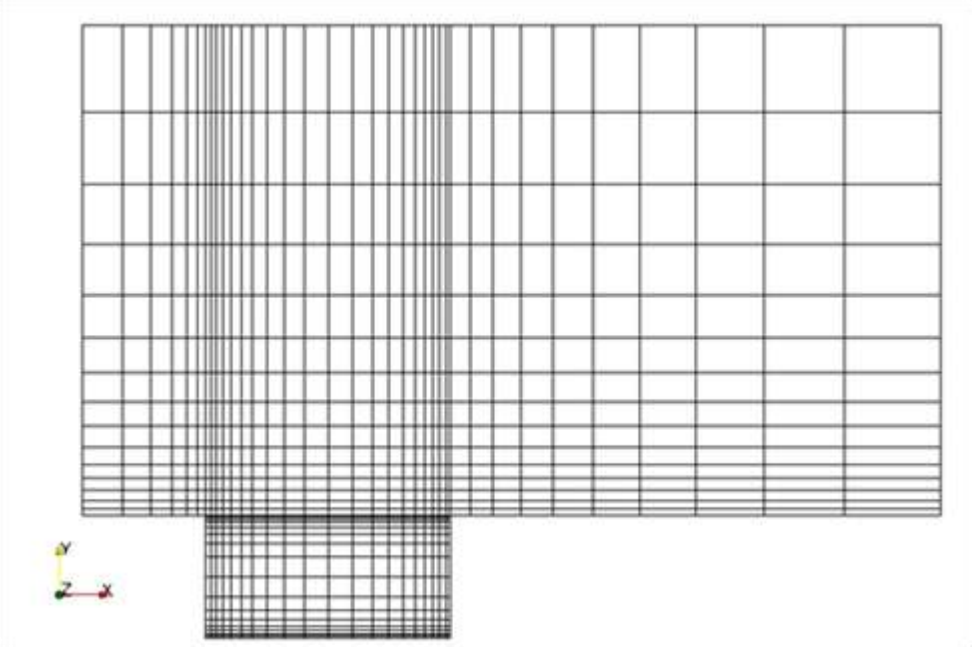

Fig 2. Computational grid of cavity in X-Y Plane

V. RESULTS AND DISCUSSIONS

5.1. Velocity Distributions

Figures 3 and 4 demonstrate the velocity vectors (as obtained from the numerical simulations for supersonic fluid flow over an open cavity) at two different instants of times such as t = 0.2 sec and t = 0.4 sec, respectively. The purpose of the velocity vector is to show the recirculation region inside the cavity. A large recirculation region exists close to the aft wall due to mass injection at high speed near the trailing edge. A small recirculation region is seen in the left bottom corner. The shocks generated at both leading and trailing edges of the open cavity can be clearly seen in the simulated results of the velocity vectors.

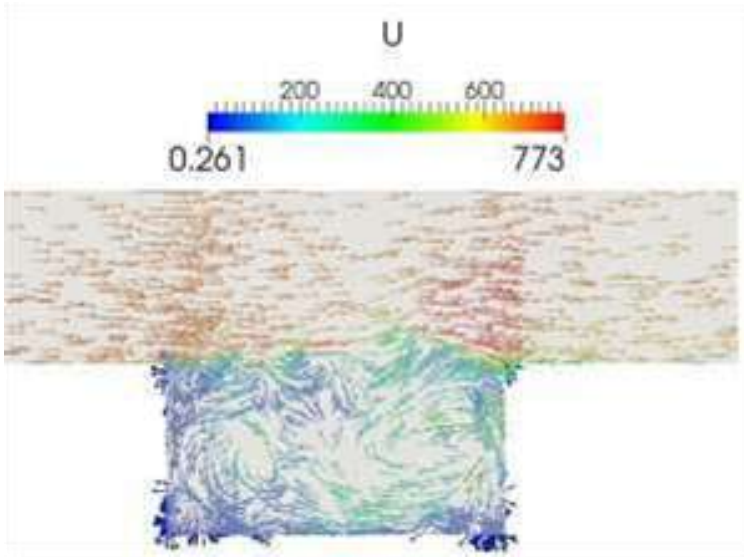

Fig 3. Velocity vector at time, t = 0.2 sec

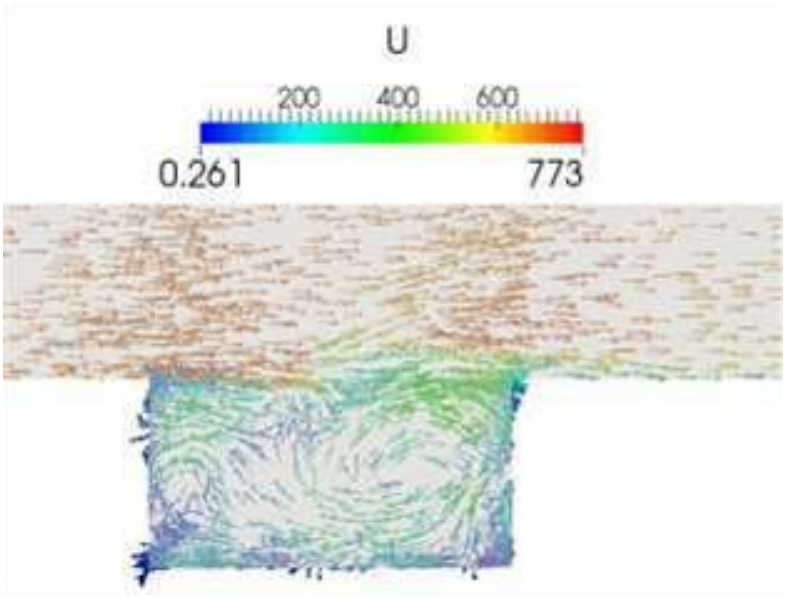

Fig 4. Velocity vector at time, t = 0.4 sec

5.2. Comparisons with other numerical and experimental results

5.2.1. Comparison of coefficient of pressure (Cp)

The comparison has been done along the side wall of the open cavity with the results of other researchers. The comparison pertaining to the coefficient of pressure (Cp) at the said cavity wall is illustrated in figure 5. Furthermore, the coefficient of pressure on the said cavity wall is found to be in both qualitative and quantitative agreement with the numerical simulation predictions available in the literature. The difference in the results from the Rizzetta's research effort is because of the difference in the Mach number.

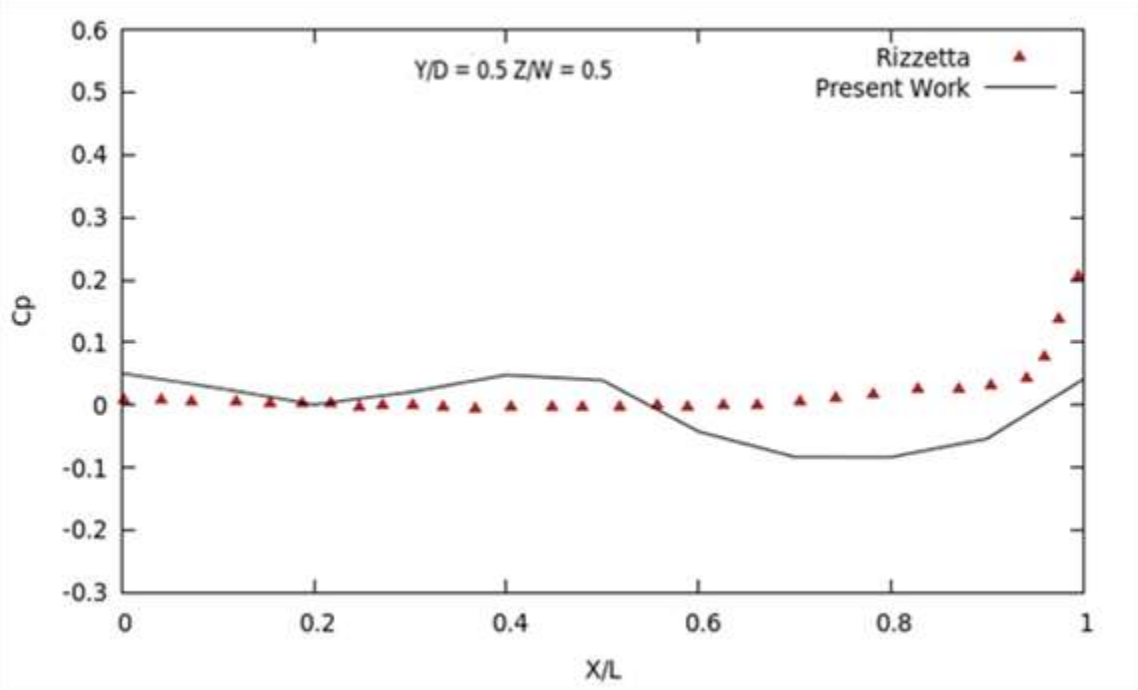

Fig 5. Coefficient of pressure along the side wall of the cavity

5.2.2. Comparison of overall sound pressure level

The comparison has also been done with the OASPL (Overall Sound Pressure Level) distributions along the side wall of the open cavity as reported by other investigators. The OASPL is denoted as:

$$OASPL = 10\,log_{10}(\overline{p_d^2}/q^2) \tag{13}$$

Where, $\overline{p_d^2} = \frac{1}{t_f - t_i}\int_{t_i}^{t_f}(p-\bar{p})^2\,dt$ (14)

q is the acoustic sound reference level with a value of 2×10^{-5} Pa

$\bar{p}$ is the time-averaged static pressure

t_f and t_i are the initial and final times, respectively

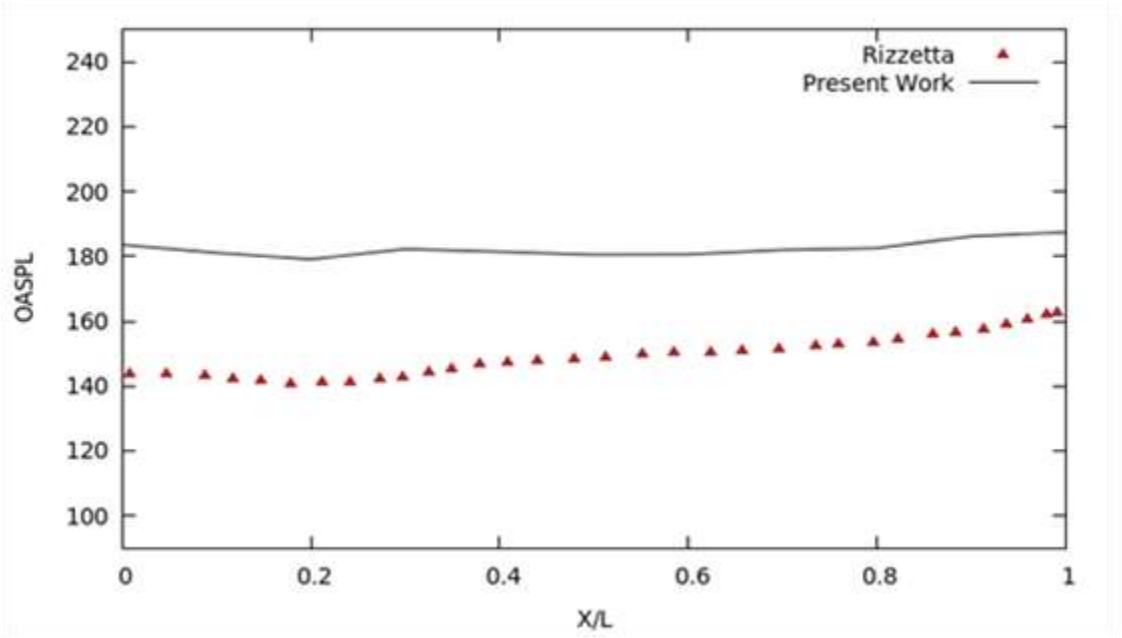

Fig 6. OASPL distribution along the side wall of the cavity

The OASPL distribution is observed to be about 33 dB higher than the Rizzetta's investigational work pertaining to the numerical predictions. The OASPL distribution at the stated cavity wall is depicted in figure 6. Additionally, the trend is very similar to the investigational works done by another researcher Rizzetta. The OASPL distribution along the side wall is over-predicted (from Rizzetta research results) by nearly 25-40 dB between the aft and front walls. Furthermore, from the current research, the predicted sound pressure level along the side wall of the cavity appears to be nearly constant throughout.

VI. CONCLUSIONS

In the current investigation work, the numerical simulations have been conducted for supersonic flow over a three-dimensional open cavity. The cavity has length-to-depth ratio of 2 and the Mach number of the free-stream is 2.0. The simulations are done by using LES based Smagorinsky model for the said cavity. The numerical simulation results are expressed in the form of both cavity flow-field and aeroacoustic analyses. Additionally, the aeroacoustic analysis is also expressed in the form of both coefficient of pressure (Cp) and overall sound pressure level (OASPL) along the side wall of the open cavity. The current numerical simulation predictions are compared with numerical simulation predictions reported in the literature. The LES model is able to predict all the main flow behaviours of the cavity. Furthermore, there is both qualitative and quantitative agreement of the coefficient of pressure with the numerical simulation results available in the literature by the other researcher for supersonic flow over the stated cavity. Alternatively, the overall sound pressure level along the side wall of the open cavity is over-predicted by 25-40 dB between the aft and front walls. In addition, the velocity vector pertaining to the cavity has also been described. Very large recirculation is observed inside the cavity and therefore these require to be reduced. Nevertheless, the attachment of a spoiler in the form of one-fourth of a cylinder at the leading edge of the cavity is also planned for future to alter the flow behaviours inside the cavity that can suppress the recirculation along with overall sound pressure level along the side wall of the cavity as well.

Acknowledgments

The author would like to thank the editor and the reviewers for extending their constructive views, valuable time and contributions for giving insightful reviews to the research article.

REFERENCES

[1] Heller, H. H., Holmes, D. G., & Covert, E. E. (1971). Flow-induced pressure oscillations in shallow cavities. Journal of sound and Vibration, 18(4), 545-553.
[2] Tam, C. K., & Block, P. J. (1978). On the tones and pressure oscillations induced by flow over rectangular cavities. Journal of Fluid Mechanics, 89(02), 373-399.
[3] Kaufman, I. I., Louis, G., Maciulaitis, A., & Clark, R. L. (1983). Mach 0.6 to 3.0 flows over rectangular cavities (No. AFWAL-TR-82-3112). Air force wright aeronautical labs wright-patterson AFB, OH.
[4] Sweby, P. K. (1984). High resolution schemes using flux limiters for hyperbolic conservation laws. SIAM journal on numerical analysis, 21(5), 995-1011.
[5] Rizzetta, D. P. (1988). Numerical simulation of supersonic flow over a three-dimensional cavity. AIAA journal, 26(7), 799-807.
[6] Anderson, J. D., & Wendt, J. F. (1995). Computational fluid dynamics (Vol. 206). New York: McGraw-Hill.
[7] Piomelli, U. (1999). Large-eddy simulation: achievements and challenges. Progress in Aerospace Sciences, 35(4), 335-362.
[8] Hamed, A., Das, K., & Basu, D. (2004). Numerical simulations of fluidic control for transonic cavity flows. AIAA Paper, 429, 2004.
[9] Li, W., Nonomura, T., Oyama, A., & Fujii, K. (2010). LES Study of Feedback-loop Mechanism of Supersonic Open Cavity Flows. AIAA paper, 5112, 2010.
[10] Vijayakrishnan, K. (2014) Unsteady RANS computations of supersonic flow over two dimensional cavity using OpenFOAM-A validation study. AIAA 2014.
[11] Sousa, R. G., et al. (2016). Lid-driven cavity flow of viscoelastic liquids**.** Journal of Non-Newtonian Fluid Mechanics, 234, 129-138, 2016.
[12] Tuerke, F., Pastur, L. R., Sciamarella, D., Lusseyran, F., & Artana, G. (2017). Experimental study of double-cavity flow. Experiments in Fluids, 76, 2017.